Statistica Sinica Preprint No: SS-2025-0356	
Title	Two Sample Testing for High-Dimensional Functional Data: A Multi-Resolution Projection Method
Manuscript ID	SS-2025-0356
URL	http://www.stat.sinica.edu.tw/statistica/
DOI	10.5705/ss.202025.0356
Complete List of Authors	Shouxia Wang, Jiguo Cao, Hua Liu, Jinhong You and Jicai Liu
Corresponding Authors	Jicai Liu
E-mails	liujicai1234@126.com
Notice: Accepted author version.	

Statistica Sinica

TWO SAMPLE TESTING FOR HIGH-DIMENSIONAL FUNCTIONAL DATA: A MULTI-RESOLUTION PROJECTION METHOD

Shouxia Wang, Jiguo Cao, Hua Liu, Jicai Liu and Jinhong You

Shanghai University of Finance and Economics, Simon Fraser University,

Xi'an Jiaotong University, Shanghai Lixin University of Accounting and Finance,

and Shanghai University of Finance and Economics

Abstract: It is of great interest to test the equality of the means in two samples of functional data. Past research has predominantly concentrated on low-dimensional functional data, a focus that may not hold in high-dimensional scenarios. In this article, we propose a novel two-sample test for the mean functions of high-dimensional functional data, employing a multi-resolution projection (MRP) method. We establish the asymptotic normality of the proposed MRP test statistic and investigate its power performance when the dimension of the functional variables is high. In practice, functional data are observed only at discrete and usually asynchronous points. We further explore the influence of function reconstruction on the test statistic theoretically. Finally, we assess the finite-sample performance of the proposed test through extensive simulation studies and demonstrate its practicality via two real data applications. Specifically, our analysis of global climate data uncovers significant differences in the functional means of climate variables in the years 2020-2069 when comparing intermediate greenhouse gas emission pathways (e.g., RCP4.5) to high greenhouse gas emission pathways (e.g., RCP8.5).

Key words and phrases: Global climate data, High-dimensional functional data, Two-sample test, Mean function, Multi-resolution projection.

1. Introduction

Over the past decade, functional data analysis (FDA) has gained significant importance in the field of statistics, primarily due to the growing demand in various disciplines to extract valuable information from complex datasets that are represented by discretized curves or surfaces. These curves or surfaces, known as functional data, are considered as random samples of functions defined over continuous domains, such as time or spatial location (Ramsay and Silverman, 2005; Ferraty and Vieu, 2006; Horváth and Kokoszka, 2012; Hsing and Eubank, 2015; Wang et al., 2016; Tang et al., 2022). Nowadays, high-resolution observations are increasingly available, which motivates high-dimensional functional data. Scientific applications are witnessing a growing amount of high-dimensional functional data, such as chemometrics, neuroscience, and climate science.

For example, in climate change research, the NASA Center for Climate Simulation (NCCS) provides projected global climate data based on two Representative Concentration Pathways (RCPs), RCP4.5 and RCP8.5. These are two scenarios that represent future greenhouse gas emission pathways (Moss et al., 2010; Thomson et al., 2011; Meinshausen et al., 2011; Chou et al., 2014), where the numerical values 4.5 and 8.5 refer to the radiative forcing produced by CO_2 emissions in 2100. RCP4.5 corresponds to an intermediate level of greenhouse gas emissions, whereas RCP8.5 signifies high emissions. Many scientists think that current emissions are tracking close to the high greenhouse gas emission RCP8.5 pathway. At present, many countries and organizations are implementing various measures to reduce emissions in order to achieve the RCP 4.5 pathway, a medium-level scenario for future greenhouse gas concentration and climate change mitigation. Thus, it is of scientific interest to test whether the climate around the whole world is different between the RCP4.5 and RCP8.5 pathways.

Each climate variable in the global climate dataset is measured across 1,028,032 geographical coordinates worldwide from 2006 to 2100. Intuitively, each climate variable measured at a specific spatial grid in a given year can be viewed as a univariate functional curve. When considering the climate variable measurements at all spatial grids for each year, we are dealing with extremely high-dimensional functional data, which has 1,028,032 dimensions. Motivated by this application, this article aims to develop a two-sample test for high-dimensional functional data to determine if the population means of two high-dimensional functional data are equal.

During the last decade, significant research efforts have focused on conducting sample testing of mean functions for functional data. For example, Cuevas et al. (2004) proposed a L_2 norm-based test for functional Analysis of Variance (ANOVA) by calculating the norms of the difference between two sample means. Ramsay and Silverman (2005) extended the classical F-test to the context of functional data by proposing a pointwise F-type test. Zhang and Liang (2014) developed a global F-type test by integrating the pointwise F-test over a specified time interval. Additionally, Horváth and Kokoszka (2012) proposed a test statistic based on the functional principal component analysis. Horváth et al. (2013) introduced two test statistics based on orthogonal projections of the difference between the mean functions. Zhang (2013) provided a comprehensive review of hypothesis testing methodologies for functional data.

All of the aforementioned tests are designed for univariate functional data. Little literature has explored two-sample tests of means for multivariate functional data. To the best of our knowledge, there is only one existing study that has investigated two-sample tests for multivariate functional data, in which the authors introduced two Hotelling T^2 type test statistics (Qiu et al., 2021). Nevertheless, it is important to note that these two Hotelling T^2 type test statistics utilizing the inverse of the sample covariance function are invalid for high-dimensional functional data because the sample covariance function is singular and inconsistent under the high-dimensional case. As far as our understanding goes, no method has been developed for testing the equality of the means for high-dimensional functional data, although extensive studies exist on testing high-dimensional mean for vector-valued data, such as Bai and Saranadasa (1996), Escanciano (2006), Chen and Qin (2010), Cai et al. (2014), Kim et al. (2020), Liu et al. (2022) and Jiang et al. (2024).

Two sample testing for high-dimensional functional data is different from that of high-dimensional vector-valued data. Due to the infinite-dimensional characteristic of functional data, the existing methods for high-dimensional vector-valued data are only suitable for each scalar component, and cannot be applied to high-dimensional functional data, where each functional variable is infinite-dimensional. In addition, for functional data or longitudinal data with asynchronous observations for different curves, the vector-based methods are not applicable. The reason is that different samples have different dimensions if treated as vectors and thus are not comparable. To tackle the problem, we develop a multi-resolution projection (MRP) technique for the first time and propose a novel MRP-based test statistic. We project the high-dimensional functional process into a one-dimensional process and then project the process into a scalar random variable. As the projection is on two different spaces, the p-dimensional vector space and the Hilbert space of square-integrable functions, we call the proposed method the multi-resolution projection. Specifically, we first define the distance between two high-dimensional random functions based on the multi-resolution projection. Next, we derive a computationally tractable form for the MRP distance and formulate the MRP test statistic. We then establish the asymptotic normality of this test statistic, which enables us to conduct hypothesis testing fast.

This article has four main contributions. Firstly, to the best of our knowledge, the proposed MRP test is the first attempt to test whether the two sample means of high-dimensional functional data are different. Secondly, the asymptotic variance of the MRP test is easily and consistently estimated, so we do not require a random permutation or bootstrap to approximate the asymptotic null distributions. Thus, the MRP test is computationally efficient. Thirdly, we explore the influence of function reconstruction on the proposed test, as we can only obtain discretized observations, which are usually asynchronous rather than continuous functions in practice. It is shown that the proposed MRP test with reconstructed functional data has the same asymptotic distribution as that with the true functions. Finally, when applied to the global climate data, we find that there are notable differences in climate characteristics between RCP4.5 and RCP8.5 over mid to long-term periods, especially in the years 2045-2069, while no significant differences are found in the years 2020-2044.

The rest of the paper is organized as follows. In Section 2.1, we introduce our test statistic through the multi-resolution projection technique. In Section 2.2, we study the asymptotic behaviors of our test statistic under the null and alternative hypotheses, as well as its power analysis. In Section 2.3, we explore the influence of function reconstruction on the proposed test theoretically. Numerical studies and real data applications are presented in Section 3 and Section 4, respectively. The conclusion is given in Section 5. All technical details are postponed to the Supplementary Material (SM).

2. Methodology and Theory

Let $\mathbf{X} = \{\mathbf{X}(t), t \in [0,1]\} = \{(X_1(t), \ldots, X_p(t))^{\mathrm{T}}, t \in [0,1]\}$ and $\mathbf{Y} = \{\mathbf{Y}(t), t \in [0,1]\} = \{(Y_1(t), \ldots, Y_p(t))^{\mathrm{T}}, t \in [0,1]\}$ be two p-dimensional random functions satisfying $\mathrm{E}\{\int_0^1 \|\mathbf{X}(t)\|_2^2 \,\mathrm{d}t\} < \infty$ and $\mathrm{E}\{\int_0^1 \|\mathbf{Y}(t)\|_2^2 \,\mathrm{d}t\} <$

∞, where the dimension p is high, X_k and Y_k each belong to $L_2([0,1])$, a Hilbert space of square-integrable functions on $[0,1]$ with the inner product $\langle f, g\rangle = \int_0^1 f(t)g(t)\,\mathrm{d}t$, $\forall f, g \in L_2([0,1])$. The mean functions of $\mathbf{X}(t)$ and $\mathbf{Y}(t)$ are defined by $\boldsymbol{\mu}_1(t) = \mathrm{E}\{\mathbf{X}(t)\}$ and $\boldsymbol{\mu}_2(t) = \mathrm{E}\{\mathbf{Y}(t)\}$, for $t \in [0,1]$. Let $\mathbf{G}_1(s,t) = \mathrm{Cov}\{\mathbf{X}(s), \mathbf{X}(t)\}$ and $\mathbf{G}_2(s,t) = \mathrm{Cov}\{\mathbf{Y}(s), \mathbf{Y}(t)\}$, for $s, t \in [0,1]$, be the covariance functions of $\mathbf{X}(t)$ and $\mathbf{Y}(t)$. We aim to test

$$H_0 : \boldsymbol{\mu}_1(t) = \boldsymbol{\mu}_2(t) \text{ for almost every } t \in [0,1] \text{ versus}$$
$$H_1 : \boldsymbol{\mu}_1(t) \neq \boldsymbol{\mu}_2(t) \text{ on a set of positive Lebesgue measure.} \tag{2.1}$$

2.1 MRP Distance Based Test

In this section, we propose a new projection-based approach to test the problem (2.1) for high-dimensional functional data. The proposed method depends on the following multi-resolution projection technique.

Lemma 1 *Let* $\mathbf{X} \in L_2^p([0,1])$ *and* $\mathbf{Y} \in L_2^p([0,1])$ *be two p-dimensional random functions, where* $L_2^p([0,1]) = L_2([0,1]) \times \cdots \times L_2([0,1])$. *Then,* $\mathrm{E}\{\mathbf{X}\} = \mathrm{E}\{\mathbf{Y}\}$ *in* $L_2^p([0,1])$ *if and only if* $\mathrm{E}\{\langle \boldsymbol{\alpha}^{\mathrm{T}}\mathbf{X}, \gamma\rangle\} = \mathrm{E}\{\langle \boldsymbol{\alpha}^{\mathrm{T}}\mathbf{Y}, \gamma\rangle\}$ *for every* $\boldsymbol{\alpha} \in \mathbb{R}^p$ *and* $\gamma \in L_2([0,1])$

Lemma 1 suggests that the test problem (2.1) is equivalent to testing the equality of expectations of the two univariate random variables $\langle \boldsymbol{\alpha}^{\mathrm{T}}\mathbf{X}, \gamma\rangle$

and $\langle \boldsymbol{\alpha}^T \mathbf{Y}, \gamma \rangle$, for every $\boldsymbol{\alpha} \in \mathbb{R}^p$ and $\gamma \in L_2([0,1])$. Note that $\langle \boldsymbol{\alpha}^{\mathrm{T}} \mathbf{X}, \gamma \rangle$ and $\langle \boldsymbol{\alpha}^T \mathbf{Y}, \gamma \rangle$ are obtained through projecting a p-dimensional random function into a random variable by the two directions $\boldsymbol{\alpha}$ and γ. Thus, we call it the multi-resolution projection approach. By Lemma 1, we define the following distance to measure the difference between $\mathrm{E}\{\mathbf{X}\}$ and $\mathrm{E}\{\mathbf{Y}\}$.

Definition 1 *Let $\mathbf{X} \in L_2^p([0,1])$ and $\mathbf{Y} \in L_2^p([0,1])$ be two p-dimensional random functions. The MRP distance of $\mathbf{X}$ and $\mathbf{Y}$ is defined by*

$$\mathit{MRP}(\mathbf{X}, \mathbf{Y}) = \int_{L_2} \int_{\mathbb{R}^p} \left(\mathrm{E}\{\langle \boldsymbol{\alpha}^{\mathrm{T}}(\mathbf{X} - \mathbf{Y}), \gamma \rangle\}\right)^2 \mathrm{d}G(\boldsymbol{\alpha}) \nu(\mathrm{d}\gamma), \tag{2.2}$$

where $G(\cdot)$ is the CDF of $\boldsymbol{\alpha}$, $G(\boldsymbol{\alpha}) = \Pi_{k=1}^p G_k(\alpha_k)$, $G_k(\alpha_k)$ is a CDF of α_k with mean 0 and variance 1, $k = 1, \ldots, p$, $\nu(\cdot)$ is the CDF of a centered process γ in $L_2([0,1])$ with a measurable, symmetric, positive definite covariance function $v(s,t)$ satisfying $\int_0^1 v(t,t)\,\mathrm{d}t < \infty$, and $\boldsymbol{\alpha}$ and γ are independent of $\mathbf{X}$ and $\mathbf{Y}$. For the identifying property below, the covariance operator $(\mathcal{V}f)(s) = \int_0^1 v(s,t) f(t)\,\mathrm{d}t$ is assumed to be injective; equivalently, $\iint f(s)f(t)v(s,t)\,\mathrm{d}s\,\mathrm{d}t > 0$ for every nonzero $f \in L_2([0,1])$.

The multi-resolution projection integral in (2.2) can be viewed as the averages over the two-direction projections with respect to the weights $G(\boldsymbol{\alpha})$ and $\nu(\gamma)$. The choice of $\boldsymbol{\alpha}$ is very flexible. For example, we can choose $\boldsymbol{\alpha} \sim N_p(0, \mathbf{I}_p)$. Note that $\mathtt{MRP}(\mathbf{X}, \mathbf{Y})$ depends on the function $v(s,t)$. In fact, by the Kolmogorov existence theorem, for any positive semi-definite function $v(s,t)$, there exists a centered Gaussian process with the covariances given by $v(s,t)$. Thus, any measurable, symmetric, positive semi-definite function $v(s,t)$ satisfying $\int_0^1 v(t,t)\,\mathrm{d}t < \infty$ can be used to define $\texttt{MRP}(\mathbf{X},\mathbf{Y})$, whereas the injectivity of $\mathcal{V}$ is needed for $\texttt{MRP}(\mathbf{X},\mathbf{Y}) = 0$ to characterize equality of the mean functions. In practice, we can choose different $v(s,t)$ based on some commonly used Gaussian processes. For example, we can consider two special choices: (i) If γ follows from a Wiener process, then $v(s,t) \propto \min\{s,t\}$. (ii) If γ is a stationary Ornstein-Uhlenbeck (OU) process, we have $v(s,t) \propto a^{-1}\exp(-a|s-t|)$, for some $a > 0$.

The proposed method is suitable for the general two-sample testing $H_0 : \boldsymbol{\mu}_1(t) - \boldsymbol{\mu}_2(t) = \boldsymbol{\mu}_0(t)$ for almost every $t \in [0,1]$ for some known $\boldsymbol{\mu}_0\,(t)$ where (2.2) should be replaced with $\texttt{MRP}(\mathbf{X},\mathbf{Y},\boldsymbol{\mu}_0) = \int_{L_2}\int_{\mathbb{R}^p}(\mathrm{E}\{\langle\boldsymbol{\alpha}^{\mathrm{T}}(\mathbf{X} - \mathbf{Y} - \boldsymbol{\mu}_0),\gamma\rangle\})^2\,\mathrm{d}G(\boldsymbol{\alpha})\nu(\mathrm{d}\gamma)$ and we need to subtract $\boldsymbol{\mu}_0(t)$ in the following (2.3). To simplify the representation, we assume $\boldsymbol{\mu}_0(t) = \mathbf{0}$.

Note that the multi-resolution projection integral in (2.2) may suffer from computational issues due to intractable integration. In the following theorem, we show that $\texttt{MRP}(\mathbf{X},\mathbf{Y})$ has a closed-form expression.

Theorem 1 *(i) Suppose that* $\mathbf{X}_1$ *and* $\mathbf{X}_2$ *are independent and identically distributed (i.i.d.) copies of* $\mathbf{X}$ *and* $\mathbf{Y}_1$ *and* $\mathbf{Y}_2$ *are i.i.d. copies of* $\mathbf{Y}$*, and* *the two collections are mutually independent. Then,*

$$\mathit{MRP}(\mathbf{X},\mathbf{Y}) = \mathrm{E}\Big\{\int_0^1\int_0^1 (\mathbf{X}_1(t)-\mathbf{Y}_1(t))^{\mathrm{T}}(\mathbf{X}_2(s)-\mathbf{Y}_2(s))\,v(s,t)\,\mathrm{d}s\,\mathrm{d}t\Big\}$$
$$= \int_0^1\int_0^1 [\boldsymbol{\mu}_1(s)-\boldsymbol{\mu}_2(s)]^{\mathrm{T}}[\boldsymbol{\mu}_1(t)-\boldsymbol{\mu}_2(t)]\,v(s,t)\,\mathrm{d}s\,\mathrm{d}t. \qquad (2.3)$$

(ii) $\mathit{MRP}(\mathbf{X},\mathbf{Y}) \geq 0$ *and* $\mathit{MRP}(\mathbf{X},\mathbf{Y}) = 0$ *if and only if* $\boldsymbol{\mu}_1(t) = \boldsymbol{\mu}_2(t)$*, for almost every* $t \in [0,1]$.

Theorem 1(i) indicates that $\mathtt{MRP}(\mathbf{X},\mathbf{Y})$ has a closed form and therefore is computationally tractable. Theorem 1(ii) implies that $\mathtt{MRP}(\mathbf{X},\mathbf{Y})$ is a reasonable measurement for the difference between the means of two random functions. We propose the following MRP test statistic based on an unbiased empirical estimate of $\mathtt{MRP}(\mathbf{X},\mathbf{Y})$:

$$\widehat{\mathtt{MRP}}(\mathbf{X},\mathbf{Y}) = \frac{1}{n(n-1)}\sum_{\substack{i,j=1\\ i\neq j}}^{n}\int_0^1\int_0^1 \mathbf{X}_i(s)^{\mathrm{T}}\mathbf{X}_j(t)v(s,t)\,\mathrm{d}s\,\mathrm{d}t$$
$$+\frac{1}{m(m-1)}\sum_{\substack{i,j=1\\ i\neq j}}^{m}\int_0^1\int_0^1 \mathbf{Y}_i(s)^{\mathrm{T}}\mathbf{Y}_j(t)v(s,t)\,\mathrm{d}s\,\mathrm{d}t$$
$$-\frac{2}{nm}\sum_{i=1}^{n}\sum_{j=1}^{m}\int_0^1\int_0^1 \mathbf{X}_i(s)^{\mathrm{T}}\mathbf{Y}_j(t)v(s,t)\,\mathrm{d}s\,\mathrm{d}t,$$

where $\{\mathbf{X}_i(t), t\in[0,1], i=1,\ldots,n\}$ and $\{\mathbf{Y}_i(t), t\in[0,1], i=1,\ldots,m\}$ are i.i.d. copies of $\mathbf{X}$ and $\mathbf{Y}$, and the two samples are mutually independent. We would reject H_0 if $\widehat{\mathtt{MRP}}(\mathbf{X},\mathbf{Y})$ is large. To derive the critical value of the proposed MRP test, we need to establish the asymptotic normality of $\widehat{\mathtt{MRP}}(\mathbf{X},\mathbf{Y})$.

2.2 Asymptotic Normality

To facilitate the presentation, we define the following notation

$$\begin{aligned}\mathtt{ITR}(\mathbf{G}_k,\mathbf{G}_j) &= \iiiint \mathrm{tr}\{\mathbf{G}_k(s,s_1)\mathbf{G}_j(t,t_1)\}\, v(s,t)v(s_1,t_1)\,\mathrm{d}s\,\mathrm{d}t\,\mathrm{d}s_1\,\mathrm{d}t_1,\\ \mathtt{IMD}(\mathbf{G}_k,\boldsymbol{\mu}_1,\boldsymbol{\mu}_2) &= \iiiint [\boldsymbol{\mu}_1(t)-\boldsymbol{\mu}_2(t)]^{\mathrm{T}}\mathbf{G}_k(s,s_1)[\boldsymbol{\mu}_1(t_1)-\boldsymbol{\mu}_2(t_1)]\\ &\qquad \times v(s,t)v(s_1,t_1)\,\mathrm{d}s\,\mathrm{d}t\,\mathrm{d}s_1\,\mathrm{d}t_1,\end{aligned}$$

where $\mathbf{G}_k(s,t)$ and $\mathbf{G}_j(s,t)$ are $p\times p$ covariance matrices for $s,t\in[0,1]$ for $k,j=1,2$. We then introduce the conditions needed.

(C1). Assume that $\mathbf{X}$ and $\mathbf{Y}$ satisfy the following general multivariate functional model:

$$\begin{aligned}\mathbf{X}_j(t) &= \boldsymbol{\mu}_1(t)+\boldsymbol{\Gamma}_1(t)\mathbf{Z}_{1j}(t), t\in[0,1],\ \text{for } j=1,\cdots,n,\\ \mathbf{Y}_j(t) &= \boldsymbol{\mu}_2(t)+\boldsymbol{\Gamma}_2(t)\mathbf{Z}_{2j}(t), t\in[0,1],\ \text{for } j=1,\cdots,m,\end{aligned}\tag{2.4}$$

where $\boldsymbol{\Gamma}_1(t)$ and $\boldsymbol{\Gamma}_2(t)$ are $p\times d$-matrices for any $t\in[0,1]$ with $d\geq p$, and $\mathbf{Z}_{ij}=\{\mathbf{Z}_{ij}(t)=(Z_{ij1}(t),\cdots,Z_{ijd}(t))^{\mathrm{T}}, t\in[0,1]\}$ is a d-dimensional random function for $i=1, j=1,\cdots,n$ and $i=2, j=1,\cdots,m$, satisfying (1) $\{\mathbf{Z}_{1j}(t)\}_{j=1}^{n}$ and $\{\mathbf{Z}_{2j}(t)\}_{j=1}^{m}$ are i.i.d. within each collection and mutually independent, with $\mathrm{E}\{\mathbf{Z}_{1j}(t)\}=\mathbf{0}$, $\mathrm{E}\{\mathbf{Z}_{2j}(t)\}=\mathbf{0}$, $\mathrm{Cov}\{\mathbf{Z}_{1j}(s),\mathbf{Z}_{1j}(t)\}=c_1(s,t)\mathbf{I}_d$, and $\mathrm{Cov}\{\mathbf{Z}_{2j}(s),\mathbf{Z}_{2j}(t)\}=c_2(s,t)\mathbf{I}_d$, where $\mathbf{I}_d$ is the $d\times d$ identity matrix, $c_1(s,t)$ and $c_2(s,t)$ are bounded for $s,t\in[0,1]$, with the corresponding normalized covariance operators $\|\mathcal{C}_1\|_{\mathcal{S}}=\iint c_1^2(s,t)\,\mathrm{d}t\,\mathrm{d}s=1$

and $\|\mathcal{C}_2\|_{\mathcal{S}} = \iint c_2^2(s,t)\,\mathrm{d}t\,\mathrm{d}s = 1$. (2) $c_1(s,t)\boldsymbol{\Gamma}_1(s)\boldsymbol{\Gamma}_1^{\mathrm{T}}(t) = \mathbf{G}_1(s,t)$ and $c_2(s,t)\boldsymbol{\Gamma}_2(s)\boldsymbol{\Gamma}_2^{\mathrm{T}}(t) = \mathbf{G}_2(s,t)$. (3)For $i=1,2$ and all j, the coordinate processes $\{Z_{ijk} : 1 \le k \le d\}$ admit jointly measurable L_2 versions. Their cross-coordinate mixed moments factorize through total order 8: for distinct $k_1,\ldots,k_q$, integers $a_1,\ldots,a_q \ge 1$ with $\sum_{\ell=1}^q a_\ell \le 8$, and $t_{\ell h} \in [0,1]$, $\mathrm{E}\{\prod_{\ell=1}^q \prod_{h=1}^{a_\ell} Z_{ijk_\ell}(t_{\ell h})\} = \prod_{\ell=1}^q \mathrm{E}\{\prod_{h=1}^{a_\ell} Z_{ijk_\ell}(t_{\ell h})\}$. Moreover, for $r = 2,3,4$ and deterministic $a_1,\ldots,a_d \in L_2([0,1])$, $\mathrm{E}|\sum_{k=1}^d \int_0^1 a_k(t) Z_{ijk}(t)\,\mathrm{d}t|^{2r} \le C_r\{\sum_{k=1}^d \iint a_k(s)c_i(s,t)a_k(t)\,\mathrm{d}s\,\mathrm{d}t\}^r$, where $C_r < \infty$.

(C2). As $\min\{m,n\} \to \infty$, $n/(m+n) \to \tau \in (0,1)$.

(C3). Assume that $\mathtt{IMD}(\mathbf{G}_k, \boldsymbol{\mu}_1, \boldsymbol{\mu}_2) = o\Big((n+m)^{-1}\mathtt{ITR}(\mathbf{G}_{12}, \mathbf{G}_{12})\Big)$, uniformly in p, for $k=1,2$, where $\mathbf{G}_{12}(s,t) = \mathbf{G}_1(s,t) + \mathbf{G}_2(s,t)$.

(C4). As $p \to \infty$, and for any $i,j,k,l \in \{1,2\}$, uniformly in p,

$$
\begin{aligned}
&|\int \cdots \int \mathrm{tr}\{\mathbf{G}_i(s,s_1)\mathbf{G}_j(t,t_1)\mathbf{G}_k(s_2,s_3)\mathbf{G}_l(t_2,t_3)\} v(s,t)v(s_1,t_1)v(s_2,t_2) \\
&\quad \times v(s_3,t_3)\,\mathrm{d}s\,\mathrm{d}t\,\mathrm{d}s_1\,\mathrm{d}t_1\,\mathrm{d}s_2\,\mathrm{d}t_2\,\mathrm{d}s_3\,\mathrm{d}t_3| = o\Big\{\Big(\mathtt{ITR}(\mathbf{G}_{12}, \mathbf{G}_{12})\Big)^2\Big\}. \qquad (2.5)
\end{aligned}
$$

Condition (C1) gives a general multivariate model for high-dimensional functional data and Chen and Qin (2010) used a similar multivariate model for high-dimensional vector-valued data. The condition $d \ge p$ means that the rank and eigenvalues of $\mathbf{G}_1(s,t)$ or $\mathbf{G}_2(s,t)$ are not affected by the transformation. Condition (C2) guarantees that m and n go to infinity proportionally, which is standard in two-sample test problems.

Condition (C3) is satisfied under H_0, and enables the variance of $\widehat{\texttt{MRP}}(\mathbf{X}, \mathbf{Y})$ to be asymptotically characterized by σ_{nm}^2 given in the following Theorem 2. Condition (C3) means that $\texttt{IMD}(\mathbf{G}_k, \boldsymbol{\mu}_1, \boldsymbol{\mu}_2)$, the difference between $\boldsymbol{\mu}_1$ and $\boldsymbol{\mu}_2$, is a smaller order of $(n+m)^{-1}\texttt{ITR}(\mathbf{G}_{12}, \mathbf{G}_{12})$. This can be interpreted as a high-dimensional version of local alternatives. To better understand Condition (C3) for high-dimensional situations, we consider a special case that $\boldsymbol{\mu}_1(t) - \boldsymbol{\mu}_2(t) = \delta(t)\mathbf{1}_p$ and $\mathbf{G}_1(s,t) = \mathbf{G}_2(s,t) = c(s,t)\mathbf{I}_p$. Then, Condition (C3) implies that $\delta(t) = o((n+m)^{-1/2})$, that is, the order of $\texttt{IMD}(\mathbf{G}_k, \boldsymbol{\mu}_1, \boldsymbol{\mu}_2)$ is $o((n+m)^{-1/2})$. For the traditional fixed p setting, the local alternative hypotheses under the above special case have the form of $\delta(t) = O((n+m)^{-1/2})$ for the classical Hotelling T^2 type test (Qiu et al., 2021), which is of larger order than the high-dimensional setting. This means that in the high-dimensional setting, we can detect smaller differences for each component than those in the fixed-dimension situation.

If Condition (C3) is not satisfied, we replace it with Condition (C3'): (C3'). Assume $(n+m)^{-1}\texttt{ITR}(\mathbf{G}_{12}, \mathbf{G}_{12}) = o\big(\texttt{IMD}(\mathbf{G}_k, \boldsymbol{\mu}_1, \boldsymbol{\mu}_2)\big)$ uniformly in p for $k = 1, 2$.

Condition (C3') means that the Mahalanobis distance between $\boldsymbol{\mu}_1(t)$ and $\boldsymbol{\mu}_2(t)$ is of a larger order than that of the left side, which can be viewed as a version of fixed alternatives. Condition (C4) is typical for establishing the asymptotic distribution by the martingale central limit theorem (Hall and Heyde, 1980). Similar conditions can be found in Chen and Qin (2010). Additionally, we do not require explicit restrictions on the relative growth rate between the dimension p and sample size n directly. The only condition on the dimension is Condition (C4). For example, Condition (C4) holds if all the eigenvalues of $\mathbf{G}_k(s,t)$ are bounded away from zero and infinity.

Theorem 2 *Under Conditions (C1)-(C4), as $p, n, m \to \infty$, we have*

$$Q(\mathbf{X},\mathbf{Y}) = \sigma_{nm}^{-1}(\mathbf{X},\mathbf{Y})\{\widehat{\mathit{MRP}}(\mathbf{X},\mathbf{Y}) - \mathit{MRP}(\mathbf{X},\mathbf{Y})\} \xrightarrow{D} N(0,1), \text{ where}$$

$$\begin{aligned}\sigma_{nm}^2(\mathbf{X},\mathbf{Y}) &= 2\{n(n-1)\}^{-1}\mathit{ITR}(\mathbf{G}_1,\mathbf{G}_1) + 2\{m(m-1)\}^{-1}\mathit{ITR}(\mathbf{G}_2,\mathbf{G}_2) \\ &\quad + 4(nm)^{-1}\mathit{ITR}(\mathbf{G}_1,\mathbf{G}_2). \end{aligned} \tag{2.6}$$

Remark 1 *If Condition (C3) is replaced by (C3'),* $\mathrm{Var}(\widehat{\mathit{MRP}}(\mathbf{X},\mathbf{Y})) = \sigma_{nm_2}^2\{1+o(1)\} = \{4n^{-1}\mathit{IMD}(\mathbf{G}_1,\boldsymbol{\mu}_1,\boldsymbol{\mu}_2)+4m^{-1}\mathit{IMD}(\mathbf{G}_2,\boldsymbol{\mu}_1,\boldsymbol{\mu}_2)\}\{1+o(1)\}$. *Theorem 2 still holds with σ_{nm} replaced by σ_{nm_2}. Under H_0, $\mathit{MRP}(\mathbf{X},\mathbf{Y}) = 0$ and Condition (C3) holds, $\sigma_{nm}(\mathbf{X},\mathbf{Y})^{-1}\widehat{\mathit{MRP}}(\mathbf{X},\mathbf{Y}) \xrightarrow{D} N(0,1)$ as $p, n, m \to \infty$.*

As the asymptotic variance $\sigma_{nm}^2(\mathbf{X},\mathbf{Y})$ defined in (2.6) is unknown, we next establish the estimation of $\sigma_{nm}^2(\mathbf{X},\mathbf{Y})$. Define for $k, j = 1, 2$, $\mathtt{TR}_{kj}(s, s_1, t, t_1) =$

$\mathrm{tr}\{\mathbf{G}_k(s,s_1)\mathbf{G}_j(t,t_1)\}$ and we can estimate $\mathtt{TR}_{kj}(s,s_1,t,t_1), k,j=1,2$ by

$$\widehat{\mathtt{TR}}_{11}(s,s_1,t,t_1) = \frac{1}{n(n-1)}\mathrm{tr}\left\{\sum_{j\neq k}^{n}[\mathbf{X}_j(s)-\overline{\mathbf{X}}_{(j,k)}(s)]\mathbf{X}_j^{\mathrm{T}}(s_1)[\mathbf{X}_k(t)-\overline{\mathbf{X}}_{(j,k)}(t)]\mathbf{X}_k^{\mathrm{T}}(t_1)\right\},$$

$$\widehat{\mathtt{TR}}_{22}(s,s_1,t,t_1) = \frac{1}{m(m-1)}\mathrm{tr}\left\{\sum_{j\neq k}^{m}\left[\mathbf{Y}_j(s)-\overline{\mathbf{Y}}_{(j,k)}(s)\right]\mathbf{Y}_j^{\mathrm{T}}(s_1)\left[\mathbf{Y}_k(t)-\overline{\mathbf{Y}}_{(j,k)}(t)\right]\mathbf{Y}_k^{\mathrm{T}}(t_1)\right\},$$

$$\widehat{\mathtt{TR}}_{12}(s,s_1,t,t_1) = \frac{1}{nm}\mathrm{tr}\left\{\sum_{j=1}^{n}\sum_{k=1}^{m}\left[\mathbf{X}_j(s)-\overline{\mathbf{X}}_{(j)}(s)\right]\mathbf{X}_j^{\mathrm{T}}(s_1)\left[\mathbf{Y}_k(t)-\overline{\mathbf{Y}}_{(k)}(t)\right]\mathbf{Y}_k^{\mathrm{T}}(t_1)\right\},$$

where $\overline{\mathbf{X}}_{(j,k)}$ (or $\overline{\mathbf{Y}}_{(j,k)}$) is the sample mean after excluding $\mathbf{X}_j$ and $\mathbf{X}_k$ (or $\mathbf{Y}_j$ and $\mathbf{Y}_k$), and $\overline{\mathbf{X}}_{(j)}$(or $\overline{\mathbf{Y}}_{(k)}$) is the sample mean without $\mathbf{X}_j$ (or $\mathbf{Y}_k$). Then, we can obtain an estimator of $\sigma^2_{nm}(\mathbf{X},\mathbf{Y})$, given by

$$\begin{aligned}\widehat{\sigma}^2_{nm}(\mathbf{X},\mathbf{Y}) &= 2\{n(n-1)\}^{-1}\widehat{\mathtt{ITR}}(\mathbf{G}_1,\mathbf{G}_1)+2\{m(m-1)\}^{-1}\widehat{\mathtt{ITR}}(\mathbf{G}_2,\mathbf{G}_2)\\ &\quad + 4(nm)^{-1}\widehat{\mathtt{ITR}}(\mathbf{G}_1,\mathbf{G}_2),\ \text{where} \qquad (2.7)\end{aligned}$$

$\widehat{\mathtt{ITR}}(\mathbf{G}_k,\mathbf{G}_j) = \iiiint \widehat{\mathtt{TR}}_{kj}(s,s_1,t,t_1)v(s,t)v(s_1,t_1)\,\mathrm{d}s\,\mathrm{d}t\,\mathrm{d}s_1\,\mathrm{d}t_1, j,k = 1,2.$ We next establish the ratio consistency of the variance estimator $\widehat{\sigma}^2_{nm}(\mathbf{X},\mathbf{Y})$.

Theorem 3 *Under Conditions (C1)-(C4), as $p,n,m\to\infty$, we have* $\widehat{\sigma}^2_{nm}(\mathbf{X},\mathbf{Y})/\sigma^2_{nm}(\mathbf{X},\mathbf{Y}) \xrightarrow{P} 1.$

Thus, $\widehat{\sigma}^2_{nm}(\mathbf{X},\mathbf{Y})$ is ratio-consistent for $\sigma^2_{nm}(\mathbf{X},\mathbf{Y})$. Note that $\mathtt{MRP}(\mathbf{X},\mathbf{Y}) = 0$ under H_0 in (2.1). By Theorems 2-3, we obtain the following result.

Corollary 1 *Under Conditions (C1)-(C4) and under H_0 in* (2.1)*, we have* $\widehat{Q}_n(\mathbf{X},\mathbf{Y}) = \widehat{\sigma}^{-1}_{nm}(\mathbf{X},\mathbf{Y})\widehat{MRP}(\mathbf{X},\mathbf{Y}) \xrightarrow{D} N(0,1),$ *as $p,n,m\to\infty$.*

By Corollary 1, the proposed MRP-based test rejects H_0 at a significance level of α if and only if $\widehat{Q}_n(\mathbf{X},\mathbf{Y}) > z_\alpha$, where z_α is the upper α quantile of $N(0,1)$. We then investigate the power of the proposed MRP test. Denote $\Delta_{nm}(\boldsymbol{\mu}_1-\boldsymbol{\mu}_2, \mathbf{G}_1, \mathbf{G}_2) = (n+m)\tau(1-\tau)\mathtt{MRP}(\mathbf{X},\mathbf{Y})/\{\sqrt{2\mathtt{ITR}(\mathbf{G}_\tau,\mathbf{G}_\tau)}\}$, where $\mathbf{G}_\tau(s,t) = (1-\tau)\mathbf{G}_1(s,t) + \tau\mathbf{G}_2(s,t)$.

Theorem 4 *Under Conditions (C1)-(C4) and under H_1 in* (2.1), *we have* $\mathrm{P}\{\widehat{Q}_n(\mathbf{X},\mathbf{Y}) > z_\alpha\} = \Phi\left\{-z_\alpha + \Delta_{nm}(\boldsymbol{\mu}_1-\boldsymbol{\mu}_2, \mathbf{G}_1, \mathbf{G}_2)\right\} + o(1)$, *where Φ is the standard normal distribution function.*

Remark 2 *The power under Condition (C3') is* $\mathrm{P}\{\widehat{Q}_n(\mathbf{X},\mathbf{Y}) > z_\alpha\} = \Phi\left(\Delta_{nm2}(\boldsymbol{\mu}_1-\boldsymbol{\mu}_2, \mathbf{G}_1, \mathbf{G}_2)\right) + o(1)$, *where* $\Delta_{nm2}(\boldsymbol{\mu}_1-\boldsymbol{\mu}_2, \mathbf{G}_1, \mathbf{G}_2) = \sqrt{(n+m)\tau(1-\tau)}\mathit{MRP}(\mathbf{X},\mathbf{Y})/\sqrt{4\mathit{IMD}(\mathbf{G}_\tau, \boldsymbol{\mu}_1, \boldsymbol{\mu}_2)}$. *This, together with Theorem 4 indicates that $\widehat{Q}_n(\mathbf{X},\mathbf{Y})$ has non-trivial power under the two alternative regimes whenever the corresponding noncentrality parameter, Δ_{nm} or Δ_{nm2}, does not vanish to 0 as $p,n,m\to\infty$.*

2.3 Influence of Function Reconstruction

In practice, continuous functional data are only observed on a series of grid points. Therefore, we need to reconstruct the true underlying function from these finite observations to compute the above test statistic. Denote the observations of X_{ik} by $\mathcal{I}X_{ik} = \{X_{ik}(t_{ik\ell}) : \ell = 1,\ldots,N_{ik}^X\}$, $i = 1,\ldots,n$,

$k = 1, \ldots, p$, and those of Y_{jk} by $\mathcal{I}Y_{jk} = \{Y_{jk}(u_{jk\ell}) : \ell = 1, \ldots, N^Y_{jk}\}$, $j = 1, \ldots, m$, $k = 1, \ldots, p$. Here $\mathcal{I}$ denotes the discretization map, and the observation grids may be asynchronous. Using these observations, the reconstructed samples are $\{\widehat{X}_{ik} = \mathcal{R}(\mathcal{I}X_{ik}) : i = 1, \ldots, n,\ k = 1, \ldots, p\}$ and $\{\widehat{Y}_{jk} = \mathcal{R}(\mathcal{I}Y_{jk}) : j = 1, \ldots, m,\ k = 1, \ldots, p\}$, where $\mathcal{R}$ is a reconstruction map, such as kernel or spline smoothing.

To ensure the effectiveness of the test, the reconstructed functional data need to satisfy the following condition:

(C5). Define $r_{X,k} = \max_{1\le i\le n} \int_0^1 \{\mathrm{E}|\widehat{X}_{ik}(t) - X_{ik}(t)|^4\}^{1/4}\,\mathrm{d}t$ and $r_{Y,k}$ analogously. Let $R_{nmp} = \sum_{k=1}^p (r_{X,k} + r_{Y,k})$. Assume that v is uniformly bounded and that the fourth moments of $X_{ik}(t)$, $Y_{jk}(t)$, $\widehat{X}_{ik}(t)$, and $\widehat{Y}_{jk}(t)$ are uniformly bounded over all indices and $t \in [0, 1]$. As $p, n, m \to \infty$, assume

$$\max_{1\le k\le p} (r_{X,k} + r_{Y,k}) = o(1), \tag{2.8}$$

$$R_{nmp} = o\{\sigma_{nm}(\mathbf{X}, \mathbf{Y})\},\ pR_{nmp} = o\{(n + m)^2\sigma^2_{nm}(\mathbf{X}, \mathbf{Y})\}. \tag{2.9}$$

In our numerical studies, we use cubic B-splines to reconstruct the random functions. For a curve observed at M points, the number of knots is set to $K_M = M^r$ for some $0 < r \le 1$, with K_M selected by generalized cross-validation. We provide some remarks on Condition (C5).

Remark 3 *Let* $N_k = \min\{\min_i N^X_{ik}, \min_j N^Y_{jk}\}$. *If each* $X_k(t)$ *and* $Y_k(t)$,

$k = 1, \ldots, p$, has bounded continuous second derivatives on $[0,1]$, then the reconstruction errors satisfy $r_{X,k}+r_{Y,k} = O(N_k^{-2r})$ and $R_{nmp} = O(\sum_{k=1}^{p} N_k^{-2r})$. Thus, $\max_k N_k^{-2r} \to 0$ implies (2.8). (i) When $\mathbf{G}_1(s,t) = \mathbf{G}_2(s,t) = c(s,t)\mathbf{I}_p$ and $\iiiint c(s,s_1)c(t,t_1)v(s,t)v(s_1,t_1)\,\mathrm{d}s\,\mathrm{d}t\,\mathrm{d}s_1\,\mathrm{d}t_1 \asymp 1$, then $\sigma_{nm}(\mathbf{X},\mathbf{Y}) \asymp p^{1/2}/n$. Thus, if $\sum_{k=1}^{p} N_k^{-2r} = o\{\min(p^{1/2}/n, 1)\}$, (2.9) holds. (ii) When $\sup_{s,s_1,t,t_1} |\operatorname{tr}\{\mathbf{G}_i(s,s_1)\mathbf{G}_j(t,t_1)\}| = O(p^{1+a})$, $i,j = 1,2$, for some $0 \leq a < 1$, and $\mathtt{ITR}(\mathbf{G}_{12},\mathbf{G}_{12}) \asymp p^{1+a}$, then $\sigma_{nm}(\mathbf{X},\mathbf{Y}) \asymp p^{(1+a)/2}/n$. Thus, if $\sum_{k=1}^{p} N_k^{-2r} = o\{\min(p^{(1+a)/2}/n, p^a)\}$, (2.9) holds.

Let $\widehat{\mathtt{MRP}}(\widehat{\mathbf{X}},\widehat{\mathbf{Y}})$ and $\widehat{\sigma}^2_{nm}(\widehat{\mathbf{X}},\widehat{\mathbf{Y}})$ be the reconstructed versions of $\widehat{\mathtt{MRP}}(\mathbf{X},\mathbf{Y})$ and $\widehat{\sigma}^2_{nm}(\mathbf{X},\mathbf{Y})$ in (2.7), by replacing the underlying curves $\{\mathbf{X}_i\}_{i=1}^n$ and $\{\mathbf{Y}_i\}_{i=1}^m$ with the reconstructed samples $\{\widehat{\mathbf{X}}_i\}_{i=1}^n$ and $\{\widehat{\mathbf{Y}}_i\}_{i=1}^m$. The following Theorem 5 establishes the asymptotic normality of $\widehat{\mathtt{MRP}}(\widehat{\mathbf{X}},\widehat{\mathbf{Y}})$.

Theorem 5 *Under Conditions (C1)-(C5), as $p,n,m \to \infty$, we have*

$$\widehat{\sigma}_{nm}^{-1}(\widehat{\mathbf{X}},\widehat{\mathbf{Y}})\big\{\widehat{\mathit{MRP}}(\widehat{\mathbf{X}},\widehat{\mathbf{Y}}) - \mathit{MRP}(\mathbf{X},\mathbf{Y})\big\} \xrightarrow{D} N(0,1).$$

By Theorem 5, we can obtain the asymptotic null distribution of $\widehat{\mathtt{MRP}}(\widehat{\mathbf{X}},\widehat{\mathbf{Y}})$.

Corollary 2 *Assume Conditions (C1)-(C5) hold. Under H_0, we have*

$$\widehat{Q}_n(\widehat{\mathbf{X}},\widehat{\mathbf{Y}}) = \widehat{\sigma}_{nm}^{-1}(\widehat{\mathbf{X}},\widehat{\mathbf{Y}})\widehat{\mathit{MRP}}(\widehat{\mathbf{X}},\widehat{\mathbf{Y}}) \xrightarrow{D} N(0,1), \text{ as } p,n,m \to \infty. \quad (2.10)$$

By the asymptotic distribution in Corollary 2, we can obtain the critical value of $\widehat{Q}_n(\widehat{\mathbf{X}}, \widehat{\mathbf{Y}})$ and test problem (2.1). Specifically, the proposed test with a nominal α level of significance rejects H_0 if $\widehat{Q}_n(\widehat{\mathbf{X}}, \widehat{\mathbf{Y}}) > z_\alpha$.

By Theorem 4 and Theorem 5, we can obtain the asymptotic power of the reconstructed test statistic $\widehat{Q}_n(\widehat{\mathbf{X}}, \widehat{\mathbf{Y}})$ as follows.

Corollary 3 *Under Conditions (C1)-(C5) and under H_1, we have*

$$\mathrm{P}\{\widehat{Q}_n(\widehat{\mathbf{X}}, \widehat{\mathbf{Y}}) > z_\alpha\} = \Phi\left(-z_\alpha + \Delta_{nm}(\boldsymbol{\mu}_1 - \boldsymbol{\mu}_2, \mathbf{G}_1, \mathbf{G}_2)\right) + o(1).$$

Corollary 3 suggests that the power of our final test statistic $\widehat{Q}_n(\widehat{\mathbf{X}}, \widehat{\mathbf{Y}})$ can converge to 1 as long as $\Delta_{nm}(\boldsymbol{\mu}_1 - \boldsymbol{\mu}_2, \mathbf{G}_1, \mathbf{G}_2) \to \infty$ as $p, n, m \to \infty$.

3. Monte Carlo Simulations

In this section, we conduct Monte Carlo simulations to assess the finite sample performance of the proposed test based on $\widehat{Q}_n(\widehat{\mathbf{X}}, \widehat{\mathbf{Y}})$. For comparison, we also consider the test method proposed by Qiu et al. (2021) (QCZ test), which includes two global test statistics: T_n by integrating a pointwise Hotelling T^2 type test statistic, and $T_{n,max}$ by taking its maximum value over $[0, 1]$. Three simulation models for $\mathbf{X}$ and $\mathbf{Y}$ are considered. The first two models are from functional moving average models, which provide a general dependent structure; the third one has sparse alternative hypotheses to illustrate the performance of our test under sparsity. We repeat each experiment 400 times and report the empirical size and power for the tests. The curves $\widehat{\mathbf{X}}, \widehat{\mathbf{Y}}$ are reconstructed by B-splines, which can be expressed by the basis functions and the corresponding coefficients. Then the integrals in the test statistic $\widehat{Q}_n(\widehat{\mathbf{X}}, \widehat{\mathbf{Y}})$ can be calculated by integrating the basis functions together with the estimated coefficients.

3.1 Simulation I

We generate data from the following functional moving average model:

$$\begin{aligned} X_{ik}(t) &= Z_{1ik}(t) + \sum_{l=1}^{p} \phi_l(t) Z_{1i(k-l)}(t) + \mu_{1k}(t), t \in [0,1]; \\ Y_{jk}(t) &= Z_{2jk}(t) + \sum_{l=1}^{p} \phi_l(t) Z_{2j(k-l)}(t) + \mu_{2k}(t), t \in [0,1], \end{aligned} \tag{3.11}$$

for $i = 1, \ldots, n$, $j = 1, \ldots, m$ and $k = 1, \ldots, p$, where $\{Z_{1ik}(t), t \in [0,1]\}_{i=1}^{n}$ and $\{Z_{2jk}(t), t \in [0,1]\}_{j=1}^{m}$ are independently generated from a standard Brownian motion defined on $[0,1]$. The coefficient functions $\phi_k(t)$s are defined as $\phi_k(t) = c_k \exp\{-t^2/2\}/\sqrt{0.7468}$, where c_ks are scalars. In the above settings, it can be seen that $\int_{[0,1]} \phi_k^2(t)\mathrm{d}t = c_k^2$. Without loss of generality, we set $\mu_{2k}(t) = 0$. We consider the following two kinds of dependence structures for $X_{ik}(t)$ and $Y_{jk}(t)$. Case I: $c_1 = 0.5$, $c_2 = 0.3$, and $c_k = 0$ for $k \geq 3$. Case II: $c_k \sim U[0.1, 0.6]$ for $k = 1, \ldots, p$.

Note that Case I presents a weaker dependence through a "two-dependence" functional moving average structure, where $X_{ik_1}(t)$ and $X_{ik_2}(t)$ (also $Y_{jk_1}(t)$ and $Y_{jk_2}(t)$) are dependent only if $|k_1 - k_2| \le 2$. In Case I, the mean function of $\mathbf{X}$ is defined by

$$\mu_{1k,\mathbf{I}}(t) = t\log(k/p+1) + \sin^2(2\pi t + k/p) + \cos(2\pi t + k/p), t \in [0,1], \quad (3.12)$$

for $k = 1, \ldots, p$. Case II presents a strong dependence through a "full-dependence" functional moving average structure, where $X_{ik_1}(t)$ and $X_{ik_2}(t)$ (also $Y_{jk_1}(t)$ and $Y_{jk_2}(t)$) are dependent if $|k_1 - k_2| \le p$. In Case II, we define the mean function of $\mathbf{X}$ by

$$\mu_{1k,\mathbf{II}}(t) = \mu_{1k,\mathbf{I}}(t)\log(p^2/2), t \in [0,1], k = 1, \ldots, p. \quad (3.13)$$

In Figure 1, we display the above mean functions $\boldsymbol{\mu}_{1,\mathbf{I}}(t) = (\mu_{11,\mathbf{I}}(t), \ldots, \mu_{1p,\mathbf{I}}(t))^{\mathrm{T}}$ and $\boldsymbol{\mu}_{1,\mathbf{II}}(t) = (\mu_{11,\mathbf{II}}(t), \ldots, \mu_{1p,\mathbf{II}}(t))^{\mathrm{T}}$ with $p = 100$.

In the following experiments, we first choose the projection process γ in (2.2) to be a stationary Ornstein-Uhlenbeck process, satisfying $v(s,t) \propto a^{-1}\exp(-a|s-t|)$ with $a = 1$. To confirm the asymptotic distribution of $\widehat{Q}_n(\widehat{\mathbf{X}}, \widehat{\mathbf{Y}})$ presented in Theorem 5, Figure 2 displays the QQ plots in Case I for model (3.11) under $n = m = 25, 40$ and $p = 20, 50, 100, 200$. From Figure 2, it can be seen that when the dimension p increases, the asymptotic distribution of $\widehat{Q}_n(\widehat{\mathbf{X}}, \widehat{\mathbf{Y}})$ is close to the standard normal distribution, which implies that the asymptotic distribution of $\widehat{Q}_n(\widehat{\mathbf{X}}, \widehat{\mathbf{Y}})$ can be well

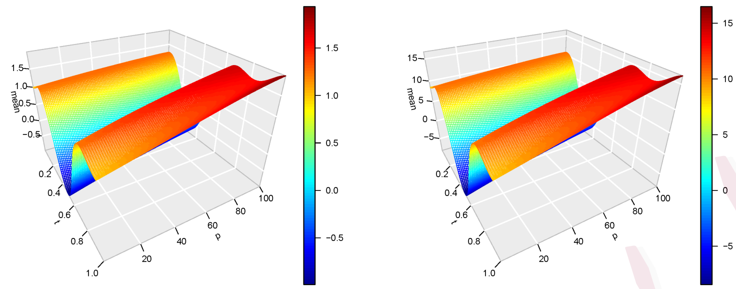

(a) $\mu_{1,\mathbf{I}}(t)$ for Case I (b) $\mu_{1,\mathbf{II}}(t)$ for Case II

Figure 1: The mean functions $\boldsymbol{\mu}_{1,\mathbf{I}}(t)$ in (3.12) and $\boldsymbol{\mu}_{1,\mathbf{II}}(t)$ in (3.13) with the dimension of functional data $p = 100$ for model (3.11) in Simulation I.

approximated by the normal distribution.

To evaluate the size and power of our method, we set $\boldsymbol{\mu}_1(t) = (\mu_{11}(t), \ldots, \mu_{1p}(t))^T$ as in Chen and Qin (2010). We vary the proportion of dimensions with $\mu_{1k}(t) = \mu_{2k}(t)$ over 0%, 50%, 75%, 90%, 95%, 98%, and 100%. The 100% case is used to assess size, and the remaining cases to assess power.

Table 1 summarizes the empirical size and power for the proposed test based on an Ornstein-Uhlenbeck process at the significance level $\alpha = 0.05$ in Cases I-II for model (3.11) under $n = m = 25, 40$ and $p = 20, 50, 100, 200$, as well as the empirical size of the two QCZ tests. Table 1 shows that the empirical sizes of our test are very close to the true significance level, which further confirms our asymptotic properties. However, the two QCZ test

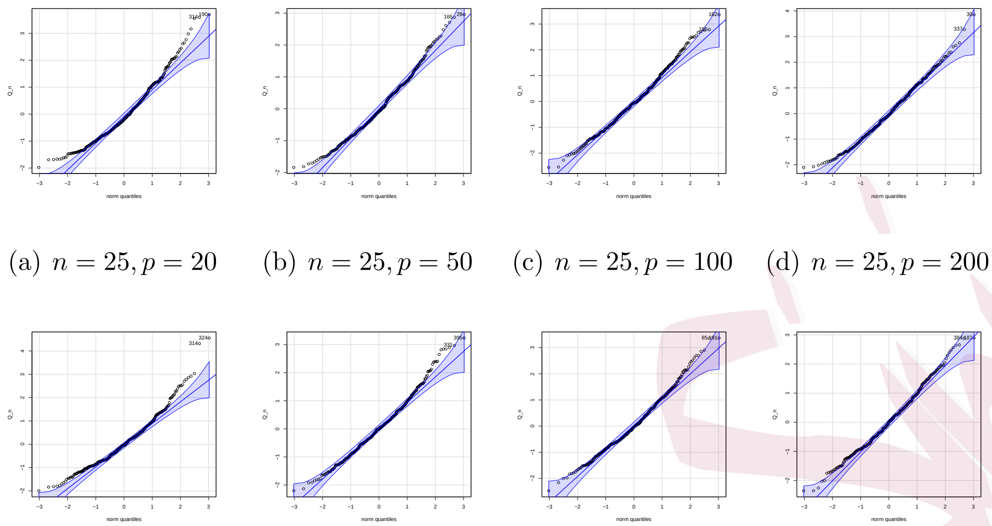

(a) $n = 25, p = 20$ (b) $n = 25, p = 50$ (c) $n = 25, p = 100$ (d) $n = 25, p = 200$

(e) $n = 40, p = 20$ (f) $n = 40, p = 50$ (g) $n = 40, p = 100$ (h) $n = 40, p = 200$

Figure 2: Q-Q plots of the MRP test statistic $\widehat{Q}_n(\widehat{\mathbf{X}}, \widehat{\mathbf{Y}})$ defined in (2.10) when $n = m = 25, 40$ and $p = 20, 50, 100, 200$ in Case I for model (3.11) in Simulation I .

statistics, T_n and $T_{n,max}$, do not achieve approximately the true significance level in most settings. Even when p is smaller than the sample sizes ($p = 20, n = m = 40$), the empirical sizes are 0.31 in Case I and 0.41 in Case II. This is perhaps because the QCZ tests are only designed for low-dimensional functional data and need to estimate the inverse of the covariance matrix, which is infeasible when functional data are high-dimensional.

Table 1 also shows that the empirical power of our test is non-trivial across all settings. Especially for $p = 50, n = m = 25$ and 98% where there is only one different component between $\boldsymbol{\mu}_1(t)$ and $\boldsymbol{\mu}_2(t)$, the power is 0.135

Table 1: The empirical size and power for the proposed MRP test and QCZ test (Qiu et al., 2021) in Cases I-II for model (3.11) at significance level $\alpha = 0.05$ in Simulation I for different (n, m) and p, where the percentages 0%, 50%, 75%, 90%, 95% 98% and 100% denote the percentages of the dimensions such that $\mu_{1k}(t) = \mu_{2k}(t)$.

			MRP test							QCZ test	
	(n, m)	p	0%	50%	75%	90%	95%	98%	100%(size)	T_n(size)	$T_{n,max}$(size)
Case I	(25, 25)	20	1	1	0.985	0.495	0.205	0.050	0.050	0.730	0.050
		50	1	1	0.995	0.785	0.435	0.135	0.050	1	0.560
		100	1	1	1	0.953	0.488	0.175	0.058	1	0.0
		200	1	1	1	0.993	0.725	0.248	0.056	1	0.0
	(40, 40)	20	1	1	0.995	0.785	0.325	0.053	0.053	0.310	0.070
		50	1	1	1	0.950	0.695	0.215	0.048	1	0.030
		100	1	1	1	1	0.855	0.295	0.054	1	0.0
		200	1	1	1	1	0.985	0.440	0.048	1	0.0
Case II	(25, 25)	20	1	1	1	1	0.998	0.050	0.050	0.720	0.040
		50	1	1	1	1	0.980	0.225	0.040	1	0.590
		100	1	1	1	1	0.695	0.195	0.056	1	0
		200	1	1	1	0.950	0.480	0.110	0.054	1	0
	(40, 40)	20	1	1	1	1	1	0.055	0.055	0.410	0.09
		50	1	1	1	1	1	0.480	0.045	1	0.06
		100	1	1	1	1	1	0.240	0.043	1	0
		200	1	1	1	1	0.860	0.143	0.052	1	0

in Case I and 0.225 in Case II. These imply that our test can effectively distinguish small differences between $\boldsymbol{\mu}_1(t)$ and $\boldsymbol{\mu}_2(t)$.

From Table 1, an interesting finding is that, for a fixed percentage of dimensions such that $\mu_{1k}(t) = \mu_{2k}(t)$, the empirical power of our test increases in Case I but decreases in Case II as p increases. This phenomenon can be explained by the theoretical analysis of the power in Theorem 4 and Corollary 3. Specifically, Theorem 4 and Corollary 3 suggest that the power is asymptotically an increasing function with respect to $\Delta_{nm}(\boldsymbol{\mu}_1 - \boldsymbol{\mu}_2, \mathbf{G}_1, \mathbf{G}_2)$. In Case I, where the covariance functions $\mathbf{G}_1$ and $\mathbf{G}_2$ allow for a two-dependence structure, when p increases, the denominator of $\Delta_{nm}(\boldsymbol{\mu}_1-$

$\boldsymbol{\mu}_2, \mathbf{G}_1, \mathbf{G}_2)$ is almost invariant, but the numerator, dependent on $\boldsymbol{\mu}_1 - \boldsymbol{\mu}_2$, becomes larger. Thus, the power becomes higher when p increases. In Case II, where the covariance functions have the full dependence structure, the denominator of $\Delta_{nm}(\boldsymbol{\mu}_1 - \boldsymbol{\mu}_2, \mathbf{G}_1, \mathbf{G}_2)$ increases faster than the signal $\boldsymbol{\mu}_1 - \boldsymbol{\mu}_2$ as p increases, yielding decreases in power.

Table 2: The empirical size and power for the proposed MRP test based on a Wiener process in Case I, Simulation I for model (3.11) at $\alpha = 0.05$ for different (n, m) and p, where 0%, 50%, 75%, 90%, 95% 98% and 100% denote the percentages of the dimensions such that $\mu_{1k}(t) = \mu_{2k}(t)$.

(n, m)	p	0%	50%	75%	90%	95%	98%	100%(size)
$(25, 25)$	20	1	1	0.900	0.330	0.165	0.043	0.043
	50	1	1	0.985	0.588	0.288	0.113	0.038
	100	1	1	0.965	0.890	0.358	0.133	0.042
	200	1	1	1	0.945	0.555	0.203	0.044
$(40, 40)$	20	1	1	0.985	0.575	0.245	0.045	0.045
	50	1	1	0.996	0.795	0.455	0.138	0.039
	100	1	1	1	0.955	0.555	0.175	0.050
	200	1	1	1	1	0.828	0.285	0.048

To examine the effect of the projection process γ on the size and power of our test, we conduct additional simulations in Case I for model (3.11) with γ a Wiener process, whose covariance satisfies $v(s, t) \propto s \wedge t := \min\{s, t\}$. Table 2 shows that the test's performance with a Wiener process is essentially similar to that with an Ornstein–Uhlenbeck process (Table 1), indicating robustness to the choice of γ. However, the Ornstein–Uhlenbeck process yields slightly higher power and is therefore recommended as the projection direction in practice.

3.2 Simulation II

The data are generated from a more complicated functional moving average structure than model (3.11), investigated by Kokoszka and Reimherr (2013):

$$\begin{aligned} X_{ik}(t) &= Z_{1ik}(t) + \sum_{l=1}^{p} \int_{[0,1]} \phi_l(u,t) Z_{1i(k-l)}(u)\mathrm{d}u + \mu_{1k}(t), t \in [0,1]; \\ Y_{jk}(t) &= Z_{2jk}(t) + \sum_{l=1}^{p} \int_{[0,1]} \phi_l(u,t) Z_{2j(k-l)}(u)\mathrm{d}u + \mu_{2k}(t), t \in [0,1], \end{aligned} \tag{3.14}$$

for $i = 1, \ldots, n$, $j = 1, \ldots, m$ and $k = 1, \ldots, p$, where $\{Z_{1ik}(t)\}_{i=1}^{n}$ and $\{Z_{2jk}(t)\}_{j=1}^{m}$ are independently generated from a standard Brownian motion defined on $[0,1]$, and $\phi_k(u,v)$s are defined as $\phi_k(u,v) = c_k \exp\{-(u^2 + v^2)/2\}/0.7468$, where c_ks are constants, satisfying $\int_{[0,1]} \int_{[0,1]} \phi_k^2(u,v)\mathrm{d}u\mathrm{d}v = c_k^2$. The norm scalar $\{c_k\}_{k=1}^{p}$ is set in the same way as Cases I-II in Simulation I. Without loss of generality, we let $\mu_{2k}(t) = 0$. The mean functions of $\mathbf{X}$ for Case I and Case II are defined by

$$\mu_{1k,\mathbf{I}}(t) = t\log(k/p+1) + \sin^2(2\pi t + k/p), \text{ for } k = 1, \ldots, p,$$

$$\mu_{1k,\mathbf{II}}(t) = \{t\log(k/p+1) + \sin^2(2\pi t + k/p)\}\log(p^2/2), \text{ for } k = 1, \ldots, p.$$

Table 3 reports the empirical size and power for the proposed test with an Ornstein-Uhlenbeck process at the significance level $\alpha = 0.05$ in Cases I-II for model (3.14). We can see that their performances are similar to those presented in Table 1 for model (3.11). The results indicate that the proposed test still works well under the more complicated functional moving average model (3.14), which generalizes Condition (C1). Thus, the proposed test is suitable for more general high-dimensional functional data with a more general version of Condition (C1). Similar to Figure 2, Figure S.1 of the SM shows the QQ plot of $\widehat{Q}_n(\widehat{\mathbf{X}}, \widehat{\mathbf{Y}})$ for Case I for model (3.14), which reveals that the asymptotic distribution of $\widehat{Q}_n(\widehat{\mathbf{X}}, \widehat{\mathbf{Y}})$ is $N(0, 1)$.

Table 3: The empirical size and power for the proposed MRP test and QCZ test (Qiu et al., 2021) in Cases I-II for model (3.14) in Simulation II at the significance level $\alpha = 0.05$ for different (n, m) and p, where the percentage 0%, 50%, 75%, 90%, 95% 98% and 100% denote the percentages of the dimensions such that $\mu_{1k}(t) = \mu_{2k}(t)$.

			MRP test							QCZ test	
	(n, m)	p	0%	50%	75%	90%	95%	98%	100%(size)	T_n(size)	$T_{n,max}$(size)
Case I	$(25, 25)$	20	1	1	0.958	0.48	0.225	0.050	0.050	0.665	0.042
		50	1	1	1	0.788	0.485	0.125	0.038	1	0.633
		100	1	1	1	0.955	0.580	0.173	0.060	1	0.0
		200	1	1	1	0.998	0.778	0.245	0.055	0.6	0.0
	$(40, 40)$	20	1	1	0.995	0.875	0.385	0.055	0.055	0.363	0.070
		50	1	1	1	0.945	0.740	0.168	0.045	1	0.058
		100	1	1	1	1	0.865	0.313	0.048	1	0.0
		200	1	1	1	1	0.985	0.483	0.048	1	0.0
Case II	$(25, 25)$	20	1	1	1	1	0.998	0.050	0.050	0.660	0.030
		50	1	1	1	1	0.988	0.280	0.055	1	0.540
		100	1	1	1	1	0.738	0.182	0.052	1	0
		200	1	1	1	0.938	0.445	0.115	0.052	1	0
	$(40, 40)$	20	1	1	1	1	1	0.053	0.053	0.370	0.08
		50	1	1	1	1	1	0.578	0.055	1	0.06
		100	1	1	1	1	0.998	0.320	0.053	1	0
		200	1	1	1	1	0.824	0.192	0.052	1	0

Similar to Table 2, Table 4 reports the empirical size and power of our test in Case I for model (3.14) at $\alpha = 0.05$ by choosing γ to be a Wiener process. The results further indicate that the Ornstein-Uhlenbeck process-based test is slightly superior to the Wiener process-based test.

Table 4: The empirical size and power for the proposed MRP test based on a Wiener process in Case I for model (3.14) in Simulation II at $\alpha = 0.05$ for different (n, m) and p, where 0%, 50%, 75%, 90%, 95% 98% and 100% denote the percentages of the dimensions such that $\mu_{1k}(t) = \mu_{2k}(t)$.

(n, m)	p	0%	50%	75%	90%	95%	98%	100%(size)
$(25, 25)$	20	1	1	0.905	0.430	0.185	0.048	0.048
	50	1	1	0.938	0.688	0.418	0.101	0.038
	100	1	1	0.959	0.845	0.482	0.133	0.059
	200	1	1	0.987	0.928	0.698	0.205	0.054
$(40, 40)$	20	1	1	0.925	0.819	0.315	0.055	0.055
	50	1	1	0.966	0.825	0.635	0.118	0.044
	100	1	1	0.988	0.925	0.785	0.223	0.048
	200	1	1	1	0.955	0.895	0.394	0.048

3.3 Simulation III

In the previous two examples, the power is relatively lower when the strengths of the signals $\mu_{2k}(t) - \mu_{1k}(t)$ under the alternatives are low relative to the level of noise. In this simulation, we further investigate the performance of our test under the sparse signal model:

$$X_{ik}(t) = Z_{1ik}(t) + \mu_{1k}(t), \quad Y_{jk}(t) = Z_{2jk}(t) + \mu_{2k}(t), \tag{3.15}$$

for $i = 1, \ldots, n$, $j = 1, \ldots, m$ and $k = 1, \ldots, p$, where $\{Z_{1ik}(t)\}_{i=1}^{n}$ and $\{Z_{2jk}(t)\}_{j=1}^{m}$ are independently generated from a standard Brownian motion defined on $[0, 1]$. Let $\mu_{1k}(t) = \varepsilon\sqrt{2\log(p)}t$ for $1 \leq k \leq q = \lfloor p^c \rfloor$, and $\mu_{2k}(t) = 0$ for $k > q$, for some $c \in (0, 1)$ and some constant ε, where c controls the sparsity of the alternative hypothesis $(\mu_{1k}(t) \neq \mu_{2k}(t) = 0)$ and ε controls the signal strength of each dimension. The alternative hypothesis is more sparse with smaller c and the signal strength of each dimension is stronger with larger ε. Table 5 summarizes the empirical size and power of our test for $p = 300$, $n = m = 25, 40$, $\varepsilon = 0.15, 0.25$ and $c = 0.35$, 0.45 and 0.55. Table 5 shows that our test can still maintain high power even in extremely sparse settings ($c = 0.35$). We also see that the power increases as c and ε increase because the strength of the signals becomes stronger. This is consistent with our theoretical power analysis.

Table 5: Empirical size and power for the MRP test based on a Wiener process for model (3.15) in Simulation III under $n = m = 25, 40$, $p = 300$, where ε controls the signal strength of each dimension, c controls the sparsity of alternative hypothesis ($\mu_{1k}(t) \neq \mu_{2k}(t)$), and q is the number of dimensions with $\mu_{1k}(t) \neq \mu_{2k}(t)$.

(n, m)	ε	$c = 0.35$ ($q = 7$)	$c = 0.45$ ($q = 13$)	$c = 0.55$ ($q = 23$)	size ($\boldsymbol{\mu}_1(t) = \boldsymbol{\mu}_2(t)$)
$(25, 25)$	0.15	0.179	0.312	0.572	0.032
	0.25	0.494	0.887	1	0.041
$(40, 40)$	0.15	0.281	0.543	0.880	0.055
	0.25	0.820	1	1	0.054

4. Real Data Analysis: Global Climate Data

In this section, we illustrate the proposed procedure by empirical analysis of two real datasets. The first dataset is the global climate data, provided by NASA Center for Climate Simulation, available at `http://ds.nccs.nasa.gov/thredds/catalog/NEX-GDDP/IND/BCSD/catalog.html`. The analysis for another application on the electroencephalogram (EEG) dataset, which concerns the relationship between genetic predisposition and the tendency for alcoholism is reported in Section S2 of the SM.

In climate change research, the RCPs are designed to provide plausible future scenarios of anthropogenic forcing, such as a low-emission scenario (RCP2.6), two intermediate scenarios (RCP4.5 and RCP6.0), and a high-emission scenario (RCP8.5). These RCP scenarios can be used in climate models for a variety of purposes such as studying the climate dynamic system and predicting future climate.

The global climate data consist of three variables: daily minimum and maximum near-surface air temperatures and daily precipitation across $1,028,032$ grid points worldwide from 2006 to 2100 under the RCP4.5 and RCP8.5 pathways. Our objective is to test whether each climate variable under RCP4.5 and RCP8.5 differs. We consider the data from 2020 to 2069 in the Arctic area, located by 360 grid points over 66.34N-89.875N and 0.125W-359.875E to analyse the climate change between RCP4.5 and RCP 8.5 pathways. There are two reasons for choosing the Arctic area. The Arctic Amplification (AA), which refers to the higher rate of warming in the Arctic than over the rest of the globe (almost twice as large as the global average) (Screen and Simmonds, 2010), is a more sensitive indicator of global climate change. Another reason is to reduce the impact of different climate types as different regions of the globe have different types of climate, with the Arctic Circle having a tundra climate. Each climate variable at 360 grid points can be viewed as a 360-dimensional functional variable. Taking the daily maximum temperature as an example, let $\mathbf{X}(t) = (X_1(t), \ldots, X_{360}(t))^{\mathrm{T}}$ and $\mathbf{Y}(t) = (Y_1(t), \ldots, Y_{360}(t))^{\mathrm{T}}$ be the daily maximum temperature over one year in RCP4.5 and RCP8.5 at the 360 grid points. Then, the samples of $\mathbf{X}(t)$ and $\mathbf{Y}(t)$ from 2020 to 2069 can be denoted as $\{\mathbf{X}_i(t)\}_{i=1}^{50}$ and $\{\mathbf{Y}_j(t)\}_{j=1}^{50}$, where each curve $\mathbf{X}_{ik}(t)$ or $\mathbf{Y}_{jk}(t)$ is observed on $N = 365$ days. Figure 3 depicts the plots of the sample mean functions of daily maximum temperature, daily minimum temperature, and daily precipitation from 2020 to 2069 for RCP4.5 and RCP8.5, respectively. We could barely recognize visually the difference in the mean functions of the daily maximum temperature, daily minimum temperature and daily precipitation between RCP4.5 and RCP8.5.

To further investigate the differences in these climatic features between RCP4.5 and RCP8.5, we apply the proposed MRP test method to analyze this dataset. Table 6 summarizes the test statistic and p-values of the proposed method for the three climate variables during three different time ranges: 2020-2069, 2045-2069, and 2020-2044. From Table 6, we can see that for the daily maximum temperature, during the entire studied time

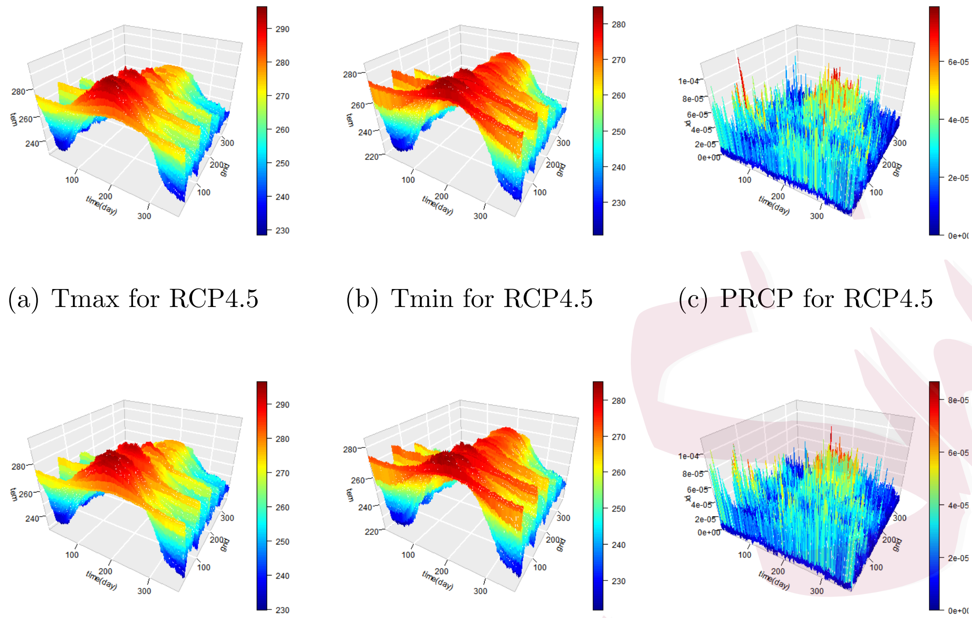

(a) Tmax for RCP4.5 (b) Tmin for RCP4.5 (c) PRCP for RCP4.5

(d) Tmax for RCP8.5 (e) Tmin for RCP8.5 (f) PRCP for RCP8.5

Figure 3: Sample means of daily maximum temperature(Tmax), daily minimum temperature(Tmin) and daily precipitation(PRCP) from 2020 to 2069 for RCP4.5 and RCP8.5.

range of 2020-2069, the p-value is almost zero, which implies that the daily maximum temperatures in the RCP4.5 and RCP8.5 pathways are different throughout the entire time range in the Arctic region. We then split the whole time range into two ranges 2020-2044 and 2045-2069 to further explore the main different periods. For the second 25 years (2045-2069), the difference in the daily maximum temperature between RCP4.5 and RCP8.5 is more significant, with a larger test statistic (15.44) than that of the whole period (5.88). However, an interesting finding is that the difference is not significant during the first 25 years (2020-2044) because of the high p-value of 0.68. For the daily minimum air temperature and daily precipitation, we can also obtain similar results. Thus, over the whole studied time range, especially the second 25 years, differences between RCP4.5 and RCP8.5 become more pronounced. These disparities may manifest as higher maximum temperatures, lower minimum temperatures, and altered patterns of precipitation. However, when examining shorter time frames, such as the first 25 years, the discrepancies between these pathways may not be statistically significant. This suggests that the effects of different greenhouse gas emission scenarios become more apparent as the time frame lengthens.

These results may be explained by the fact that emissions peak around 2045 under the lower emission pathway RCP4.5, while carbon emissions have been growing under the higher emission pathway RCP8.5. The findings suggest that implementing effective measures to reduce carbon emissions would have a positive impact on climate conditions. Taking action promptly to decrease greenhouse gas emissions is crucial for mitigating climate change and its associated risks. To achieve significant carbon emission reductions, a combination of measures is necessary, including transitioning to renewable energy, improving energy efficiency, adopting sustainable transportation methods, promoting circular economy practices, and implementing nature-based solutions. Governments, organizations, and individuals need to work together to implement these measures and ensure a sustainable future for generations to come.

Table 6: Testing the difference of the mean functions of the projected global climate data based on two Representative Concentration Pathways (RCP4.5 and RCP8.5) by the proposed MRP test method.

Climate Variable	Time Range	(n, m, p)	Test Statistic	p-value
Daily Maximum Temperature	2020-2069	(50,50,360)	5.88	2.00×10^{-9}
	2045-2069	(25,25,360)	15.44	$< 10^{-16}$
	2020-2044	(25,25,360)	-0.48	0.684
Daily Minimum Temperature	2020-2069	(50,50,360)	5.47	2.25×10^{-8}
	2045-2069	(25,25,360)	14.88	$< 10^{-16}$
	2020-2044	(25,25,360)	0.067	0.473
Daily Precipitation	2020-2069	(50,50,360)	2.36	9.14×10^{-3}
	2045-2069	(25,25,360)	2.71	3.36×10^{-3}
	2020-2044	(25,25,360)	1.61	0.0537

5. Conclusions and Discussion

This paper proposes a new multi-resolution projection approach to detect the difference between two mean functions of high-dimensional functional data. We derive the asymptotic properties of the proposed test statistic under the null and alternative hypotheses. The influence of the reconstruction of the functional curves on our test is also explored as observations are discretized in practice which are usually asynchronous. The usefulness of the proposed methods has been demonstrated by simulation studies and two real datasets.

This paper focuses on densely observed functional data. Zhu and Wang (2023) considered a two-sample test for equality of distributions for sparsely measured functional data and proposed a test of marginal homogeneity by adapting to a sampling plan. An interesting future direction is to study the two-sample test for the sparse high-dimensional functional data. Recently, two-sample tests for equality of distributions have gained more and more attention in the literature of functional data, see Wynne and Duncan (2022) and Zhu and Wang (2023). Using our multi-resolution projection technique to deal with this problem is also worthwhile to study.

Supplementary Materials

We provide additional simulation and real data analysis results, and technical details in the Supplementary Material.

Acknowledgements

Shouxia Wang's research was supported by National Natural Science Foundation of China (NSFC) (No.72501165). Jiguo Cao's research was supported by Natural Sciences and Engineering Research Council of Canada

Discovery grant (RGPIN-2023-04057). Hua Liu's research was supported by the NSFC (No.12201487). Jinhong You's research was supported by the 111-Center Project of China (No. B25066). The corresponding authors are Jicai Liu and Jinhong You (co-corresponding).

References

Bai, Z. D. and H. Saranadasa (1996). Effect of high dimension: By an example of a two sample problem. *Statistica Sinica 6*(2), 311–329.

Cai, T., W. Liu, and Y. Xia (2014). Two-sample test of high dimensional means under dependence. *Journal of the Royal Statistical Society Series B 76*(2), 349–372.

Chen, S. X. and Y. L. Qin (2010). A two-sample test for high-dimensional data with applications to gene-set testing. *The Annals of Statistics 38*(2), 808–835.

Chou, S. C., A. Lyra, C. Mourão, C. Dereczynski, I. Pilotto, J. Gomes, J. Bustamante, P. Tavares, A. Silva, and D. Rodrigues (2014). Assessment of climate change over South America under RCP 4.5 and 8.5 downscaling scenarios. *American Journal of Climate Change 3*(05), 512.

Cuevas, A., M. Febrero, and R. Fraiman (2004). An ANOVA test for functional data. *Computational Statistics & Data Analysis 47*(1), 111–122.

Escanciano, J. C. (2006). A consistent diagnostic test for regression models using projections. *Econometric Theory 22*(6), 1030–1051.

Ferraty, F. and P. Vieu (2006). *Nonparametric Functional Data Analysis: Theory and Practice.* New York: Springer.

Hall, P. and C. C. Heyde (1980). *Martingale Limit Theory and its Application.* Probability and Mathematical Statistics. New York: Academic Press.

Horváth, L. and P. Kokoszka (2012). *Inference for Functional Data with Applications.* New York: Springer.

Horváth, L., P. Kokoszka, and R. Reeder (2013). Estimation of the mean of functional time series and a two-sample problem. *Journal of the Royal Statistical Society Series B 75*(1), 103–122.

Hsing, T. and R. Eubank (2015). *Theoretical Foundations of Functional Data Analysis, with an Introduction to Linear Operators.* Chichester: John Wiley & Sons.

Jiang, Y., X. Wang, C. Wen, Y. Jiang, and H. Zhang (2024). Nonparametric two-sample tests of high dimensional mean vectors via random integration. *Journal of the American Statistical Association 119*(545), 701–714.

Kim, I., S. Balakrishnan, and L. Wasserman (2020). Robust multivariate nonparametric tests via projection averaging. *The Annals of Statistics 48*(6), 3417–3441.

Kokoszka, P. and M. Reimherr (2013). Determining the order of the functional autoregressive model: Order of functional autoregression. *Journal of Time Series Analysis 34*, 116–129.

Liu, W., X. Yu, and R. Li (2022). Multiple-splitting projection test for high-dimensional mean vectors. *Journal of Machine Learning Research 23*(71), 1–27.

Meinshausen, M., S. J. Smith, K. Calvin, J. S. Daniel, M. L. Kainuma, J.-F. Lamarque, K. Matsumoto, S. A. Montzka, S. C. Raper, and K. Riahi (2011). The RCP greenhouse gas concentrations and their extensions from 1765 to 2300. *Climatic Change 109*, 213–241.

Moss, R. H., J. Edmonds, K. A. Hibbard, M. R. Manning, S. K. Rose, D. P. van Vuuren, T. R. Carter, S. Emori, M. Kainuma, T. Kram, G. A. Meehl, J. F. B. Mitchell, N. Nakicenovic, K. Riahi, S. J. Smith, R. J. Stouffer, A. M. Thomson, J. P. Weyant, and T. J. Wilbanks (2010). The next generation of scenarios for climate change research and assessment. *Nature 463*, 747–756.

Qiu, Z., J. Chen, and J. Zhang (2021, May). Two-sample tests for multivariate functional data with applications. *Computational Statistics & Data Analysis 157*, 107160.

Ramsay, J. O. and B. W. Silverman (2005). *Functional Data Analysis*. Springer, New York.

Screen, J. A. and I. Simmonds (2010). The central role of diminishing sea ice in recent arctic temperature amplification. *Nature 464*(7293), 1334–1337.

Tang, C., H. L. Shang, and Y. Yang (2022). Clustering and forecasting multiple functional time series. *The Annals of Applied Statistics 16*(4), 2523–2553.

Thomson, A. M., K. V. Calvin, S. J. Smith, G. P. Kyle, A. Volke, P. Patel, S. Delgado-Arias, B. Bond-Lamberty, M. A. Wise, and L. E. Clarke (2011). RCP4.5: a pathway for stabilization of radiative forcing by 2100. *Climatic Change 109*, 77–94.

Wang, J.-L., J.-M. Chiou, and H.-G. Müller (2016). Functional data analysis. *Annual Review of Statistics and Its Application 3*, 257–295.

Wynne, G. and A. B. Duncan (2022). A kernel two-sample test for functional data. *Journal of Machine Learning Research 23*(73), 1–51.

Zhang, J. (2013). *Analysis of Variance for Functional Data.* Chapman and Hall, New York.

Zhang, J. and X. Liang (2014). One-way ANOVA for functional data via globalizing the pointwise F-test. *Scandinavian Journal of Statistics 41*(1), 51–71.

Zhu, C. and J. L. Wang (2023). Testing homogeneity: the trouble with sparse functional data. *Journal of the Royal Statistical Society Series B 85*(3), 705–731.

Shouxia Wang, School of Statistics and Data Science, Shanghai University of Finance and Economics; E-mail: wangshouxia@sufe.edu.cn

Jiguo Cao, Department of Statistics and Actuarial Science, Simon Fraser University; E-mail: jiguo_cao@sfu.ca

Hua Liu, School of Economics and Finance, Xi'an Jiaotong University; E-mail: liuhua_22@xjtu.edu.cn

Jicai Liu, School of Statistics and Mathematics, Shanghai Lixin University of Accounting and Finance; E-mail: liujicai1234@126.com

Jinhong You, School of Statistics and Data Science, Shanghai University of Finance and Economics; E-mail: johnyou07@163.com